feedback gain parameter k_i can be construed as a distinct advantage of the new proportional-integral control law derived in this Note.

V. Conclusions

The main contribution of Note is the design of a new class of angular velocity-free attitude stabilization controllers that can be viewed as generalizations of the existing passivity-based control algorithms in the sense of providing an additional provision for integral feedback action. Through a rigorous Lyapunov analysis, we have demonstrated global asymptotic stability for the full state of the rigid-body rotational motion when the external disturbances are absent. The disturbance rejection aspect is illustrated using a linearized setting of the problem. The controller structure includes a low-pass linear filter state that is derived without explicit differentiation of attitude to synthesize angular velocity-like signals. Numerical implementation of these new results provide the assurance of significantly improved steady-state attitude error convergence in the presence of constant unknown external disturbances as a result of integral feedback action. Whereas in this study we have adopted the once-redundant Euler parameter representation for the attitude kinematics, the main results presented here can be readily replicated in terms of other kinematic representations derived from the Euler principal rotation theorem such as the Gibbs vector and the modified Rodrigues parameters.

Acknowledgments

These results are based in part upon work supported by the Texas Advanced Research Program under Grant 003658-0081-2001.

References

[1]Junkins, J. L., and Turner, J. D., *Optimal Spacecraft Rotational Maneuvers*, Elsevier Science, Amsterdam, 1986, Chap. 8.

[2]Schaub, H., and Junkins, J. L., *Analytical Mechanics of Space Systems*, AIAA Education Series, AIAA, Reston, VA, 2003, Chap. 8.

[3]Lizarralde, F., and Wen, J. T., "Attitude Control Without Angular Velocity Measurement: A Passivity Approach," *IEEE Transactions on Automatic Control,* Vol. 41, No. 3, 1996, pp. 468–472.

[4]Tsiotras, P., "Further Passivity Results for the Attitude Control Problem," *IEEE Transactions on Automatic Control*, Vol. 43, No. 11, 1998, pp. 1597–1600.

[5]Akella, M. R., "Rigid Body Attitude Tracking Without Angular Velocity Feedback," *Systems and Control Letters*, Vol. 42, No. 4, 2001, pp. 321–326.

[6]Akella, M. R., and Kotamraju, G. R., "Rigid-Body Output Feedback Attitude Control Subject to Actuator and Rate Saturations," *14th US Congress on Theoretical and Applied Mechanics*, U.S. National Committee on Theoretical and Applied Mechanics, 2002.

[7]Subbarao, K., "The Attitude Control Problem, Re-Visited," Advances in the Astronautical Sciences, The John L. Junkins Astrodynamics Symposium, Vol. 115, Univelt, San Diego, CA, 2003, pp. 95–110.

[8]Paielli, R. A., and Bach, R. E., "Attitude Control with Realization of Linear Error Dynamics," *Journal of Guidance, Control, and Dynamics*, Vol. 16, No. 1, 1993, pp. 182–189.

[9]Shuster, M. D., "A Survey of Attitude Representations," *Journal of the Astronautical Sciences*, Vol. 41, No. 4, 1993, pp. 439–517.

[10]Stanley, W. S., "Quaternion from Rotation Matrix," *Journal of Guidance and Control*, Vol. I, No. 3, 1978, pp. 223, 224.

[11]Burg, D., Dawson, J. H., and de Queiroz, M. S., "An Adaptive Partial State Feedback Controller For RLED Robot Manipulators," *IEEE Transactions of Automatic Control*, Vol. 41, No. 7, 1996, pp. 1024–1031.

[12]Wong, H., de Querioz, M. S., and Kapila, V., "Adaptive Tracking Control Using Synthesized Velocity From Attitude Measurements," *Automatica*, Vol. 37, No. 6, 2001, pp. 947–953.

[13]Ortega, R., Loria, A., Nicklasson, P. J., and Ramirez, H., *Passivity-Based Control of Euler-Lagrange Systems*, Springer-Verlag, New York, 1998.

[14]Ioannou, P. A., and Sun, J., *Stable and Robust Adaptive Control*, Prentice–Hall, Upper Saddle River, NJ, 1995, pp. 85–134, Chaps. 2–4.

Lyapunov-Based Nonlinear Missile Guidance

N. Léchevin*
Université du Québec à Trois-Rivières, Trois-Rivières, Quebec G9A 5H7, Canada
and
C. A. Rabbath†
Defence Research and Development Canada–Valcartier, Val-Belair, Quebec G3J 1X5, Canada

I. Introduction

PROPORTIONAL navigation guidance (PNG) has been widely used for decades because of its implementation simplicity and its effectiveness in guiding missiles to intercept nonmaneuvering targets.[1] Recently, new guidance laws have been proposed, based mainly on optimal control theory,[2,3] differential game theory,[4] the geometric approach,[5] and variable structure control[6] to meet the challenges posed by ever more agile targets. Improvements to PNG have also been proposed. For instance, neoclassical guidance[7,8] requires line-of-sight (LOS) rate measurements only to warrant zero-miss distance by rendering the kinematics-PNG-seeker-missile dynamic loop positive real. Novel guidance laws are often obtained in the context of linear systems theory. The argument for such linear synthesis is that small-angle engagement justifies linearization around an operating point and, in particular, around a null LOS rate. However, for the pursuit of highly maneuverable targets and to satisfy demanding precision guidance requirements, synthesis of guidance laws considering the nonlinear missile–target relative kinematics is intuitively expected to provide performance superior to that of a linear design relying on approximations. Nonlinear guidance laws providing performance improved over that of classical PNG have recently been proposed.[9,10] In this context, an issue arising with the selection of the Lyapunov function candidate relates to the guidance law potentially depending on terms such as $1/\cos(\lambda)$, where λ is the LOS angle.[10] The commanded acceleration may then become prohibitively large around LOS angles close to $\pm\pi/2$ rad. In this Note, we propose a quadratic Lyapunov function candidate resulting in guidance laws that are free of singularities, such as $\lambda = \pm\pi/2$ rad; and that provide reduced miss distances when compared to PNG. The cornerstone of the proposed approach lies in the particular selection of the state-space variables used in the Lyapunov-based synthesis, which are trigonometric functions of the LOS and LOS rate. Provided certain conditions are met, the proposed approach warrants uniform ultimate boundedness of the missile–target system state, namely LOS and LOS rate, for the case of highly maneuvering targets. For nonmaneuvering targets, asymptotic stability is demonstrated. Numerical simulations show the effectiveness of the proposed nonlinear guidance laws.

II. Mathematical Preliminaries

A. Missile–Target Kinematics

A two-dimensional engagement can be studied by assuming that the lateral and longitudinal planes are decoupled.[8] The engagement

Received 27 February 2004; revision received 15 June 2004; accepted for publication 6 July 2004.

*Adjunct Professor, Department of Electrical Engineering; Nicolas_Lechevin@uqtr.ca.

†Defence Scientist, 2459 Pie-XI N.; camille-alain.rabbath@drdc-rddc.gc.ca.

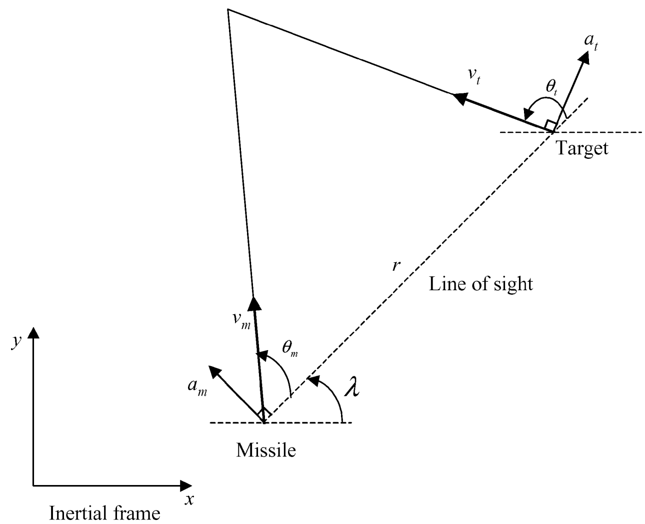

Fig. 1 Engagement geometry—collision triangle.

geometry is shown in Fig. 1, where $v_m \in \mathcal{R}$ and $a_m \in \mathcal{R}$ are missile speed and normal acceleration, respectively, and $v_t \in \mathcal{R}$ and $a_t \in \mathcal{R}$ are target speed and normal acceleration, respectively. The range r between missile and target is related to closing velocity v_{cl} as $v_{\mathrm{cl}} = -\dot{r}$. The LOS angle $\lambda(t)$ is related to the missile–target relative separation $y(t)$ as $\sin[\lambda(t)] = y(t)/r(t)$.

Reference to the independent time variable t is omitted unless stated otherwise. Differentiating the expression for the relative separation twice yields the following missile–target kinematics:

$$\begin{bmatrix} \cos(\lambda) & 0 \\ -\dot{\lambda}\sin(\lambda) & \cos(\lambda) \end{bmatrix} \begin{bmatrix} \dot{\lambda} \\ \ddot{\lambda} \end{bmatrix} = \begin{bmatrix} \dfrac{\dot{y}r - y\dot{r}}{r^2} \\ f(r, \dot{r}, \ddot{r}, \lambda, \dot{\lambda}, a_t, a_m) \end{bmatrix}$$

$$\ddot{y} = a_t - a_m \tag{1}$$

with

$$f(r, \dot{r}, \ddot{r}, \lambda, \dot{\lambda}, a_t, a_m) = [a_t - a_m - 2\dot{\lambda}\dot{r}\cos(\lambda) - \ddot{r}\sin(\lambda)]/r \tag{2}$$

B. Assumptions

Assumption 1 (Measurements): The synthesis presented in this note assumes deterministic signals exempt from noise. Sensor dynamics are assumed to be significantly faster than missile–target dynamics so that they can be omitted; that is, the rate gyros, the accelerometers, and the seeker dynamics are assumed to have unity gains.

Assumption 2 (Target Behavior): Although only normal accelerations are considered in this note, three target behaviors are studied.

Case 1: No maneuver; that is, $a_t = 0$.

Case 2: Maneuvering target with estimates $\hat{a}_t(t)$ available to the guidance law as delayed target accelerations; that is, $\hat{a}_t(t) = a_t(t - \tau)$, where $\tau \in \mathcal{R}^+$. With the target acceleration bounded as $|a_t(t)| < \overline{a_t}/2$, where $\overline{a_t} \in \mathcal{R}$, then $|\hat{a}_t(t) - a_t(t)| < \overline{a_t}$.

Case 3: Constant normal acceleration $a_t = a_t^0 \in \mathcal{R}$, null tangential acceleration, and constant closing velocity v_{cl}.

With unknown target maneuvers, a variable-structure, multiple-model target state estimator (constant speed and acceleration[11] models) can be employed. Such an estimator would allow discrimination among the guidance laws and selection of the most appropriate one and would lead to a multiple-model control approach.[12]

Assumption 3 (Missile–Target Range): Range r and the first two time derivatives of the range are bounded as follows:

$$r_m < r < r_M, r_m, r_M \in \mathcal{R}$$

$$|\dot{r}| < r_M^v \in \mathcal{R}, \qquad |\ddot{r}| < r_M^a \in \mathcal{R} \tag{3}$$

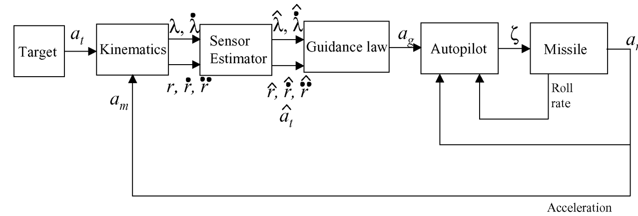

Fig. 2 Structure of nonlinear missile guidance.

The first inequality (3) is needed to avoid singularities when the range becomes relatively small and to confine the range to a maximum value. This is a reasonable assumption, as warheads are typically detonated by the trigger action of a proximity fuze. In general, the smallest miss distance r_m is set to half the largest target dimension. It should be noted, however, that the value of r_m affects the closed-loop pole placement and, consequently, the ultimate bound on the missile–target state trajectories. Therefore, a tradeoff between physically achievable transient dynamics and largest acceptable miss distance has to be made by the designer. Such a tradeoff may be constrained, in part, by the particular warhead and fuzing components installed in the missile. The second and third inequalities (3) express the limitations in velocities and accelerations of both the missile and the target. For the missile, maneuverability is constrained by its aerodynamics.

C. Guidance Objectives

The objective of the guidance law is to drive the missile to the collision triangle[1] shown in Fig. 1, satisfying the following condition:

$$v_t \sin(\theta_t) = v_m \sin(\theta_m) \tag{4}$$

Equation (4) corresponds to the equilibrium $\dot{\lambda} = 0$ for system (1). The guidance command a_g is synthesized so that system (1) is asymptotically stable at equilibrium $(\lambda = \lambda_o, \dot{\lambda} = 0)$. Figure 2 shows the general feedback structure for the guidance system, which includes the dynamics of a maneuvering target, the missile flight-control system, and an estimator.

III. Lyapunov-Based Nonlinear Guidance

A. Lyapunov Function Candidate

The flight-control-system dynamics are assumed to be ideal; that is, $a_g = a_m$. In other words, the missile-flight-control-system dynamics are assumed to be significantly faster than those of the guidance loop. Define the following state variables:

$$x_1 = \sin(\lambda) - \sin(\lambda_o), \qquad x_2 = \dot{x}_1 \tag{5}$$

where λ_o represents a fixed LOS angle at equilibrium. Angle λ_o can be specified by the designer to achieve a missile–target impact at a specific angle, that is, with $\lambda_o = \lambda + \theta_t + \beta$, where β is a desired offset angle.[13] As an example of a situation where λ_o has a prescribed value, optimal guidance laws that include λ and $\dot{\lambda}$ in feedback are sometimes used[14] to stabilize the system around $\lambda_o = 0$ and $\dot{\lambda} = 0$. Such techniques are known to be robust against uncertain time-to-go. Alternatively, λ_o can be interpreted as a kinematic constraint imposed on the missile–target behavior until intercept. Defining the state variables as in Eq. (5) is a key step of the proposed synthesis. Indeed, using trigonometric functions of the LOS angle λ and its derivative rather than using λ and $\dot{\lambda}$ directly, as recently proposed,[10] no singularity in λ is present in the expressions for the Lyapunov function candidate and the guidance law. Differentiating Eq. (5) yields

$$\dot{x}_1 = \dot{\lambda}\cos(\lambda), \qquad \dot{x}_2 = \ddot{\lambda}\cos(\lambda) - \dot{\lambda}^2\sin(\lambda) \tag{6}$$

From Eq. (5), system (1) can be formulated with the following state-space representation:

$$\begin{bmatrix}\dot{x}_1\\ \dot{x}_2\end{bmatrix} = \underbrace{\begin{bmatrix}0 & 1\\ 0 & 0\end{bmatrix}}_{=A}\underbrace{\begin{bmatrix}x_1\\ x_2\end{bmatrix}}_{=x} + \underbrace{\begin{bmatrix}0\\ 1\end{bmatrix}}_{=B} f(r,\dot{r},\ddot{r},\lambda,\dot{\lambda},a_t,a_m)$$

$$x_1(t_0) = \sin[\lambda(t_0)] - \sin(\lambda_0), \qquad x_2(t_0) = \dot{\lambda}(t_0)\cos[\lambda(t_0)] \tag{7}$$

where t_0 is initial time (defined as zero in this Note). For brevity and for clarity of demonstration, suppose that the guidance law is devised using target acceleration estimate $\hat{a}_t$ and exact values for the range, its derivatives, the LOS, and the LOS rate. A state-feedback guidance law can thus be formulated as

$$\mu_g = r\cdot g(r,\dot{r},\ddot{r},\lambda,\dot{\lambda},\hat{a}_t) - r\underbrace{[k_1 \quad k_2]}_{=K}\begin{bmatrix}x_1\\ x_2\end{bmatrix} \tag{8}$$

with

$$g(r,\dot{r},\ddot{r},\lambda,\dot{\lambda},a_t) = a_t/r - 2\dot{\lambda}(\dot{r}/r)\cos(\lambda) - (\ddot{r}/r)\sin(\lambda) \tag{9}$$

and where $N > 0$ and the first term on the right-hand side of the equality corresponds to proportional navigation weighted by $\cos(\lambda)$. Because $\mu_g = a_m$, one can write the state-feedback system as

$$\dot{x} = [A + B(K + K_r)]x + (B/r)(a_t - \hat{a}_t) \tag{10}$$

with

$$K_r = \begin{bmatrix}0 & -\dfrac{Nv_{\mathrm{cl}}}{r}\end{bmatrix} \tag{11}$$

To determine K, the following Lyapunov function candidate is proposed:

$$V(x_1,x_2) = \tfrac{1}{2}x^TPx \tag{12}$$

where P is a symmetric positive definite matrix and $x^T = [x_1 \;\; x_2]$. The time derivative of $V(x_1,x_2)$ can be expressed as

$$\dot{V}(x_1,x_2) = \tfrac{1}{2}x^T[P(A+BK) + (A^T + K^TB^T)P]x$$
$$+ x^TPB[(a_t - \hat{a}_t)/r] \tag{13}$$

Because (A, B) forms a controllable pair, K can be selected so that the eigenvalues of $(A+BK)$ are in the left half of the complex plane. Consequently, there exists a symmetric positive definite matrix Q such that

$$P(A+BK) + (A^T + K^TB^T)P = -Q \tag{14}$$

and Eq. (13) can be written as

$$\dot{V}(x_1,x_2) = -\tfrac{1}{2}x^TQx + x^T(PB/r)(a_t - \hat{a}_t) \tag{15}$$

Remark: To reach a conclusion about the stability of the missile–target system, which is represented by the state $(\lambda,\dot{\lambda})$, from the behavior of the trajectory given by the state (x_1,x_2), the LOS angle equilibrium must take the following values: $\lambda_o \in \mathcal{R}\backslash\{-\pi/2,\pi/2\}$. This is to avoid singularity in the state transformation. However, there is no singularity problem with the guidance law μ_g at these values of λ_o.

B. Consideration of Case 1

For a nonmaneuvering target, $a_t = 0$, target acceleration estimates are set to $\hat{a}_t = 0$. From Eq. (15),

$$\dot{V}(x_1,x_2) = -\tfrac{1}{2}x^TQx \tag{16}$$

and asymptotic stability is guaranteed because the Lyapunov function candidate decreases on the trajectories x of system (7).

C. Consideration of Case 2

For a maneuvering target with delayed estimates $\hat{a}_t(t)$ available to the guidance law, the derivative of the Lyapunov function candidate given by Eq. (15) is bounded, using Assumption 2, as

$$\dot{V}(x_1,x_2) \le -\tfrac{1}{2}x^TQx + \|x^TPB\|(\bar{a}_t/r_m) \tag{17}$$

Note that variable structure estimation $\hat{a}_t$ based on knowledge of the bound $\bar{a}_t$ leads to asymptotic stability. However, the chattering inherent in this approach is undesirable in practical implementations. Reducing chattering by boundary-layer techniques is possible and is known to result in ultimately bounded state trajectories.[15] In the present paper, the authors have opted for a linear matrix inequalities (LMI) characterization of the pole placement problem.[16] The choice of a gain matrix K such that $(A+BK)$ has all of its eigenvalues with real parts to the left of $-h < 0$ can be expressed as

$$P(A+BK) + (A^T + K^TB^T)P + 2hP < 0 \tag{18}$$

Then, when Eq. (14) is replaced by relation (18), relation (17) becomes

$$\dot{V}(x_1,x_2) \le -\lambda_m^P\cdot h\cdot\|x\|^2 + \left(\bar{a}_t\sigma_M^P/r_m\right)\|x\| \tag{19}$$

where σ_M^P and λ_m^P are the largest singular value and the smallest eigenvalue of $P > 0$, respectively, and $\|\cdot\|$ is the Euclidian norm of its argument. Let $\theta \in (0, 1)$; then

$$\dot{V}(x_1,x_2) \le -(1-\theta)\lambda_m^Ph\|x\|^2 \qquad \text{for} \qquad \|x\| > \frac{\sigma_M^P\bar{a}_t}{\theta\lambda_m^Phr_m} \tag{20}$$

The system is then uniformly ultimately bounded[13]; that is, trajectories (x_1,x_2) enter a ball $B_1(O, b_1)$ centered at $O = (0, 0)$ and having radius b_1 given as

$$b_1 = \frac{\sigma_M^P\bar{a}_t}{\theta\lambda_m^Phr_m}\sqrt{\frac{\lambda_M^P}{\lambda_m^P}} \tag{21}$$

where λ_M^P is the largest eigenvalue of P. The compact set B_1 to which the system trajectories (x_1,x_2) converge can be reduced by increasing h, that is, by selecting new static feedback gains according to relation (18) that correspond to the eigenvalues of $(A+BK)$ being farther to the left of the complex plane. However, there exists a tradeoff between the selection of a relatively small radius b_1, and hence of the smallest upper bound of the final value of (x_1,x_2), and the admissible control effort. It should be noted that a value of b_1 close to zero induces a near-zero miss distance as (x_1,x_2) approach zero. Ideally, the selection of b_1 should take into account the potential saturation of fin deflection. Clearly, simulation tests must be performed to determine values satisfying a reasonable tradeoff.

D. Consideration of Case 3

For constant a_t and v_{cl}, integral control is added to the state feedback to provide steady-state input tracking. This is done as follows: let $\hat{a}_t = 0$ and

$$\mu_g = r\cdot g(r,\dot{r},\ddot{r},\lambda,\dot{\lambda},0) + \mu_g^o \tag{22}$$

where μ_g^o is some state-feedback strategy, and rewrite the system in (7) as

$$\begin{bmatrix}\dot{x}_1\\ \dot{x}_2\end{bmatrix} = \begin{bmatrix}0 & 1\\ 0 & 0\end{bmatrix}\begin{bmatrix}x_1\\ x_2\end{bmatrix} + \begin{bmatrix}0\\ 1\end{bmatrix}\frac{\left(a_t - \mu_g^o\right)}{r} \tag{23}$$

Perform the change of variables $\dot{z}_2 = r \cdot \dot{x}_2$, $\dot{z}_1 = z_2$ and let the state-feedback control μ_g^o be given as

$$\mu_g^o = -K_p z - k_i \int_0^t z_1(\tau)\,\mathrm{d}\tau \tag{24}$$

where $K_p = [k_1 \;\; k_2]$ and $z^T = [z_1 \;\; z_2]$. By differentiating Eq. (23), the system dynamics become

$$\begin{bmatrix} \dot{z}_1 \\ \dot{z}_2 \\ \dot{z}_3 \end{bmatrix} = \begin{bmatrix} 0 & 1 & 0 \\ 0 & 0 & 1 \\ k_i & k_1 & k_2 \end{bmatrix} \begin{bmatrix} z_1 \\ z_2 \\ z_3 \end{bmatrix} \tag{25}$$

With a proper choice of K_p and k_i, Eq. (25) can be made asymptotically stable. As z_1 is the integral of z_2, only z_2 has to be computed. Note that

$$\int_0^t \dot{z}_2\,\mathrm{d}\tau = z_2 - z_2(0) = r\dot{x}_1 + v_{\mathrm{cl}} x_1 - r(0)\dot{x}_1(0) - v_{\mathrm{cl}} x_1(0) \tag{26}$$

Primitive function z_2 of $\dot{z}_2$ can be defined as

$$z_2 = r\dot{x}_1 + v_{\mathrm{cl}} x_1 \qquad \text{for all} \qquad t \geq 0 \tag{27}$$

Integration of Eq. (27) gives

$$z_1 - z_1(0) = r x_1 + 2 v_{\mathrm{cl}} \int_0^t x_1\,\mathrm{d}\tau - r x_1(0) \tag{28}$$

A possible choice for z_1 is

$$z_1 = r x_1 + 2 v_{\mathrm{cl}} \int_0^t x_1\,\mathrm{d}\tau \qquad \text{for all} \qquad t \geq 0 \tag{29}$$

Note that

$$z_3 = r\ddot{x}_1 \tag{30}$$

Adopt the following change of variables to obtain state trajectories in x for stability analysis:

$$\xi_1 = \int_0^t x_1(\tau)\,\mathrm{d}\tau, \qquad \xi_2 = \dot{\xi}_1 (= x_1), \qquad \xi_3 = \dot{\xi}_2 (= x_2) \tag{31}$$

Then

$$\dot{\xi}_1 = (z_1 - 2v_{\mathrm{cl}}\xi_1)/r, \qquad \dot{\xi}_2 = (z_2 - v_{\mathrm{cl}}\xi_2)/r, \qquad \dot{\xi}_3 = z_3/r \tag{32}$$

From Eq. (25), the gain vector K_p and scalar gain k_i can be chosen such that there exists an arbitrarily large constant $\alpha \in \mathcal{R}^+$ and such that the derivative of the Lyapunov function

$$U(z_1, z_2, z_3) = \left(z_1^2 + z_2^2 + z_3^2\right)/2 \tag{33}$$

is expressed as

$$\dot{U}(z_1, z_2, z_3) = -\alpha\left(z_1^2 + z_2^2 + z_3^2\right) \tag{34}$$

Consider the Lyapunov function candidate

$$W(\xi_1, \xi_2, \xi_3) = \left(\xi_1^2 + \xi_2^2 + \xi_3^2\right)/2 \tag{35}$$

then the derivative of W augmented by $\dot{U}$ yields

$$\begin{aligned}\dot{U} + \dot{W} = &\left(-\alpha z_1^2 + \xi_1 z_1/r - 2v_{\mathrm{cl}}\xi_1^2/r\right) \\ &+ \left[(-\alpha/2)z_2^2 + \xi_2 z_2/r - (v_{\mathrm{cl}}/2r)\xi_2^2\right] \\ &+ \left[(-\alpha/2)z_2^2 + z_2 z_3/r^2 - (\alpha/2)z_3^2\right] \\ &+ \left[(-v_{\mathrm{cl}}/2r)\xi_2^2 - \left(v_{\mathrm{cl}}/r^2\right)\xi_2 z_3 - (\alpha/2)z_3^2\right]\end{aligned} \tag{36}$$

By completing the squares, Eq. (36) can be written as

$$\begin{aligned}\dot{U} + \dot{W} = &(-2v_{\mathrm{cl}}/r)(\xi_1 - z_1/4v_{\mathrm{cl}})^2 + z_1^2/8v_{\mathrm{cl}}r - \alpha z_1^2 \\ &-(v_{\mathrm{cl}}/2r)(\xi_2 - z_2/v_{\mathrm{cl}})^2 + z_2^2/2v_{\mathrm{cl}}r - (\alpha/2)z_2^2 \\ &-(\alpha/2)\left(z_3 - z_2/\alpha r^2\right)^2 + z_2^2/2\alpha r^4 - (\alpha/2)z_2^2 \\ &-(v_{\mathrm{cl}}/2r)(\xi_2 + z_3/r)^2 + v_{\mathrm{cl}}z_3^2/2r^3 - (\alpha/2)z_3^2\end{aligned} \tag{37}$$

Thus, $\dot{U} + \dot{W}$ is negative definite, given that α is selected so that

$$\alpha > \max\left(v_{\mathrm{cl}}/r_m^3,\, 1/r_m^2,\, 1/v_{\mathrm{cl}}r_m\right) \tag{38}$$

Provided inequality (38) is met, the system is stable along the trajectories (ξ_2, ξ_3) and hence along (x_1, x_2).

Remark: Case 2 is about a target having constant velocity amplitude moving along a circular trajectory. In this case, the tangential acceleration is null and the normal acceleration is constant with value v_t^2/ρ_m, where ρ_m is the radius of curvature of the target trajectory. From basic missile–target kinematics,

$$\|v_m\| = \frac{\|v_t\|\cos(\theta_t) + \|v_{\mathrm{cl}}\|}{\cos(\theta_m)} \tag{39}$$

where $\|v_t\|$ and $\|v_{\mathrm{cl}}\|$ are constant by Assumption 2. The guidance law $\mu_g = a_m$ is in fact devised to compensate for the effect of a constant normal acceleration a_t. Then, from Eq. (39), a time-varying v_m arises from the guidance law μ_g which forces the LOS and the LOS rate to attain an equilibrium point; this in turn affects θ_t and θ_m so that they reach a certain value with time.

E. Proposed Guidance: A Summary

Proposition 1: Stabilizing nonlinear guidance laws for the missile–target system (7–9) are given as follows for the three target behaviors investigated:

Case 1 (Nonmaneuvering Target): The state-feedback guidance law of Eq. (8) using Lyapunov function candidate (12) to solve for the state-feedback gain.

Case 2 (Maneuvering Target): The state feedback with LMIs, to solve for the feedback gain, and the Lyapunov function candidate derivative which is bounded as in equality (17).

Case 3 (Constant Target Acceleration and Closing Velocity): Integral control combined with state feedback, as given in Eq. (22), where gain is solved by using the Lyapunov function candidates Eqs. (33) and (35).

The guidance laws associated with cases 1 and 3 result in asymptotic stability of the system (7–9) at $(\lambda_o, 0)$, where $\lambda_o \in \mathcal{R}\backslash\{-\pi/2, \pi/2\}$ strictly for the purpose of stability analysis, whereas the guidance law associated with case 2 results in uniform boundedness of the system trajectories.

Remark: During the homing phase, v_{cl} can be taken as quasi-constant and positive; then adding the term $\mu_g^{\mathrm{png}} = N v_{\mathrm{cl}}\dot{\lambda}\cos(\lambda)$ with $N > 0$ in the expression for μ_g introduces the damping term $-(N v_{\mathrm{cl}}/r_m)x_2^2 < 0$ in the time derivative of the Lyapunov function. Collecting terms in $\dot{\lambda}$ in $\mu_g + \mu_g^{\mathrm{png}}$ gives $(N+2)v_{\mathrm{cl}}\dot{\lambda}\cos(\lambda)$, which is equivalent to the well-known PNG law for small angles ($\cos(\lambda) \simeq 1$).

IV. Numerical Simulations

Consider the second-order flight control system dynamics given as

$$a_m/a_g = 1/(s^2/\omega^2 + 2\xi s/\omega + 1) \tag{40}$$

and the first-order LOS rate measurement

$$\frac{[\mathrm{d}\lambda_m/\mathrm{d}t](s)}{\lambda(s)} = \frac{s}{s+\tau_s} \tag{41}$$

In Eqs. (40) and (41), λ_m is the measured LOS angle and the parameter values are

$$\omega = 20 \text{ rad/s}, \qquad \xi = 0.707, \qquad \tau_s = 0.1 \text{ s} \tag{42}$$

The block diagram of the missile-control system is shown in Fig. 3. Simulations are performed with and without the saturator block.

A. Constant Target Acceleration and Closing Velocity

Case 3 of Proposition 1 is simulated. Flight times are given by $t_f \in \{2, 2.5, 3, 3.5, \ldots, 10\}$ in seconds, $a_t = 100$ m/s^2, and $v_{\mathrm{cl}} = 1000$ m/s. The missile-to-target range is given by $r = v_c(t_f - t)$ and $\mathrm{d}^2r/\mathrm{d}t^2 = 0$. Three guidance laws are simulated: 1) the proposed nonlinear state-feedback plus, the PNG guidance law given by Eq. (8) and labeled as NLPNG with $\dot{r} = \ddot{r} = 0$, $k_1 = -4.5 \times 10^{-2}$, $k_2 = -0.3$; 2) the proposed nonlinear state-feedback plus PNG and integration guidance law (denoted as NLPNG + INT) given by Eqs. (22) and (24), with $k_i = -2.33 \times 10^{-2}$, $K_p = -[1.94 \;\; 7.20] \times 10^{-1}$, and $\ddot{\lambda}$, used in the computation of x_2, is expressed as

$$\ddot{\lambda} = \frac{s}{s+\tau_s/10}\left[\frac{\mathrm{d}\lambda_m}{\mathrm{d}t}\right](s) \tag{43}$$

and 3) the classical PNG law given by

$$a_g = 5v_c\frac{\mathrm{d}\lambda_m}{\mathrm{d}t} \tag{44}$$

For each value of t_f, the missile control system of Fig. 3 is simulated and the miss-distances $y(t_f)$ are calculated. Figure 4 shows the miss distances. The proposed nonlinear guidance laws result in the smallest miss distances for each t_f considered. In particular, NLPNG + INT offers the best performance among the methods tested because NLPNG + INT compensates for the effect of the constant exogenous disturbance (target acceleration) applied to the missile–target system, which is not the case with NLPNG and PNG. It should be noted that the synthesis of the guidance laws NLPNG and NLPNG + INT is carried out assuming idealized missile and sensor dynamics; however, the numerical simulations involve more realistic first- and second-order ODEs. Figure 5 demonstrates the missile accelerations obtained with the various guidances for $t_f = 10$ s and $a_t = 100$ m/s^2.

B. Maneuvering Target

Case 2 of Proposition 1 is simulated. Target acceleration is given by $a_t = 10g\sin(1.7t)$ m/s^2, where $g = 9.81$ m/s^2. The performance

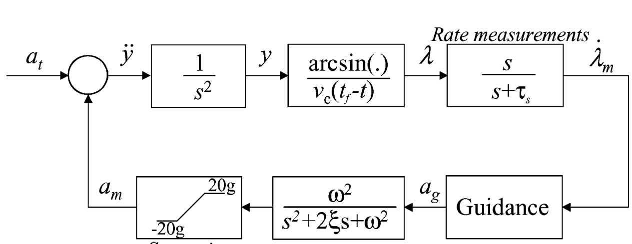

Fig. 3 Missile control system used in the simulations.

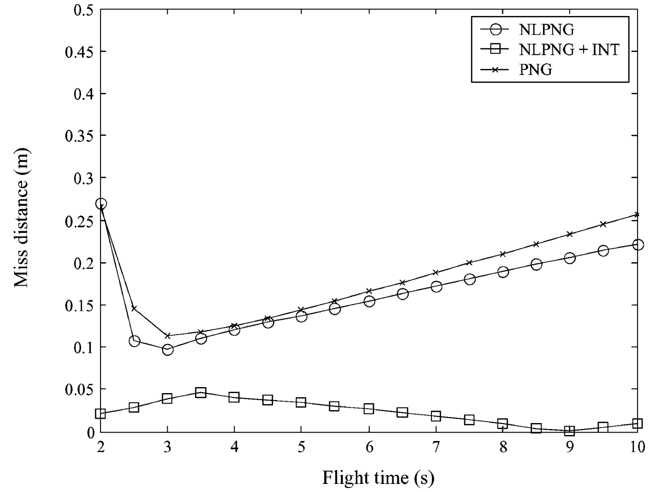

Fig. 4 Miss distances (a_t = 100 m/s^2).

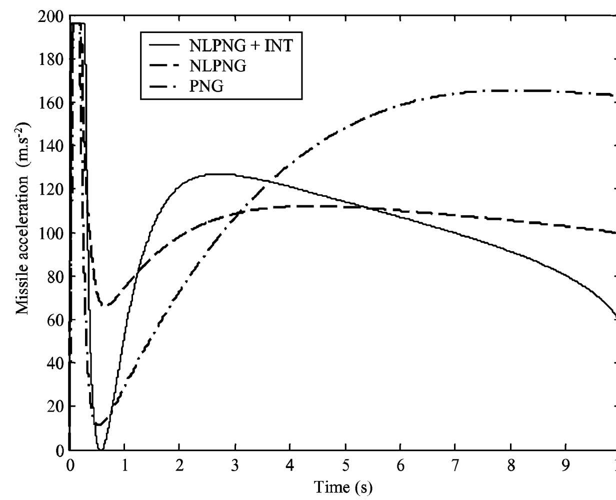

Fig. 5 Missile accelerations vs time.

of the proposed NLPNG is compared with those of the classical PNG and the optimal guidance[2,7] law (OGL) given by

$$a_g(t) = \frac{N(t_{\mathrm{go}})}{t_{\mathrm{go}}^2}\left[y(t) + t_{\mathrm{go}}\cdot\frac{\mathrm{d}y(t)}{\mathrm{d}t} + 0.5\hat{a}_t(t)\cdot t_{\mathrm{go}}^2 - a_m(t)\cdot\left(e^{-t_{\mathrm{go}}} + t_{\mathrm{go}} - 1\right)\right] \tag{45}$$

$$N(t_{\mathrm{go}}) = \frac{6t_{\mathrm{go}}^2\left(e^{-t_{\mathrm{go}}} + t_{\mathrm{go}} - 1\right)}{2t_{\mathrm{go}}^3 - 6t_{\mathrm{go}}^2 + 6t_{\mathrm{go}} + 3 - 12t_{\mathrm{go}}e^{-t_{\mathrm{go}}} - 3e^{-2t_{\mathrm{go}}}}$$

$$\hat{a}_t(t) = a_t(t-0.2), \qquad t_{\mathrm{go}} = t_f - t \tag{46}$$

where $\hat{a}_t(t)$ is a delayed estimate of the target acceleration and t_{go} is time-to-go. The same delayed acceleration estimate is used for the implementation of NLPNG. Figure 6 show the miss distances vs flight times with and without saturation. When the saturator block is included in the loop, OGL and NLPNG give similar miss distances, which are smaller than those obtained with classical PNG. However, when the saturator block is excluded, OGL provides the smallest miss distance. Importantly, because of its asymptotic stability property, the proposed guidance law results in relatively large missile accelerations at the beginning of flight, during the transient phase, and settles to smaller amplitudes toward the end of the engagement, as shown in Fig. 7 for $t_f = 10$ s and $a_t = 10g\sin(1.7t)$ m/s^2. This is as opposed to OGL and PNG, which result in increased demands in acceleration towards the end of the pursuit. Hence, the proposed

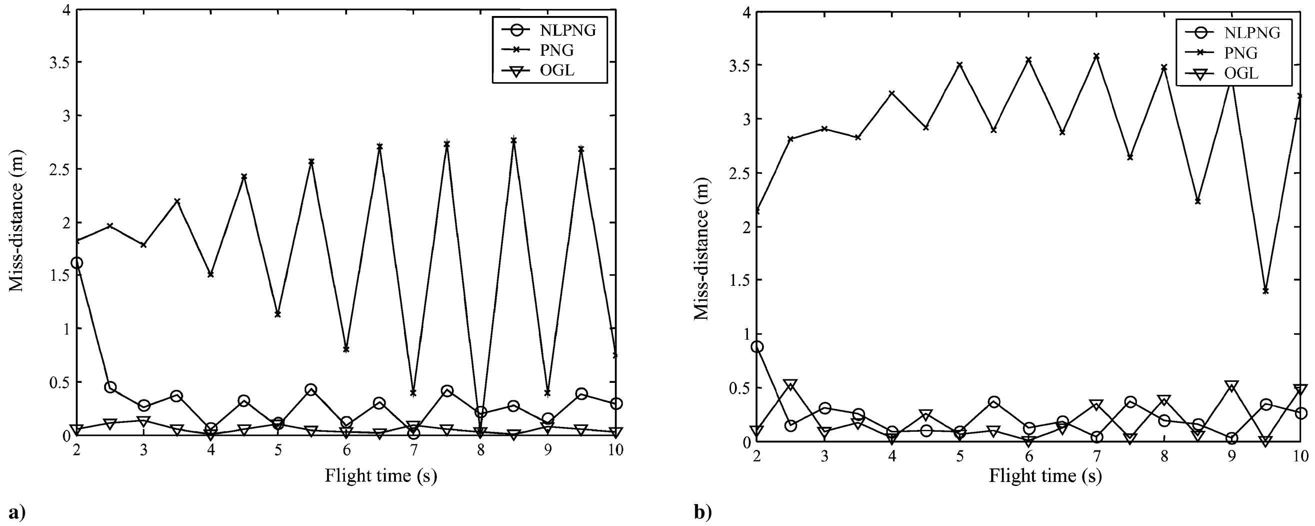

Fig. 6 Miss-distances ($a_t = 10g \sin(1.7t)$ m/s^2): a) without and b) with saturation.

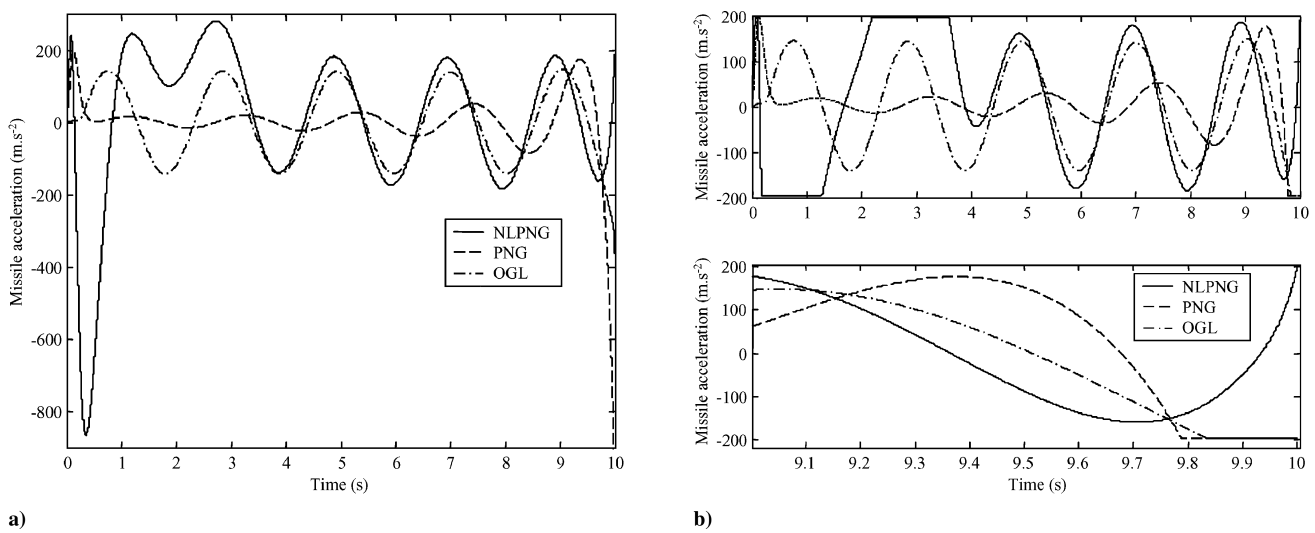

Fig. 7 Missile accelerations vs time: a) without and b) with saturation.

NLPNG results in the miss distance being less sensitive to saturation than OGL and PNG. Another key feature of NLPNG is that its implementation is simpler than that for OGL, making it more appealing for real-time computations.

V. Conclusions

This Note proposed a new Lyapunov function candidate for the synthesis of nonlinear guidance laws, which are free of singularities, and for the stability analysis of missile–target systems considering the whole state. The Note also studied the behavior of the proposed nonlinear guidance laws for three classes of target maneuvers: 1) no maneuver, 2) maneuvering target with estimates of target acceleration available as delayed signals, and 3) constant normal acceleration and closing velocity and null tangential acceleration. It was shown that uniform ultimate boundedness of the missile–target system trajectory is obtained in the case of highly maneuvering targets, for which a delayed, bounded acceleration estimate is assumed to exist. For nonmaneuvering targets and targets having a constant acceleration, asymptotic stability was obtained and demonstrated. The work presented in this note is currently being extended to the synthesis of nonlinear guidance laws taking into account uncertain missile dynamics.

References

[1]Zarchan, P., *Tactical and Strategic Missile Guidance*, Vol. 199, Progress in Astronautics and Aeronautics, AIAA, Reston, VA, 2002, pp. 11–29.

[2]Cottrel, R. G., "Optimal Intercept Guidance for Short-Range Tactical Missiles," *AIAA Journal*, Vol. 9, No. 7, 1971, pp. 1414, 1415.

[3]Rusnak, I., and Meir, L., "Optimal Guidance for High-Order and Acceleration Constrained Missile," *Journal of Guidance, Control, and Dynamics*, Vol. 14, No. 3, 1991, pp. 589–596.

[4]Gutman, S., "On Optimal Guidance for Homing Missiles," *Journal of Guidance, Control, and Dynamics*, Vol. 2, No. 4, 1979, pp. 296–300.

[5]Chiou, Y. C., and Kuo, C. Y., "Geometric Approach to Three-Dimensional Missile Guidance Problem," *Journal of Guidance, Control, and Dynamics*, Vol. 21, No. 2, 1998, pp. 335–341.

[6]Moon, J., Kim, K., and Kim, Y., "Design of Missile Guidance Law via Variable Structure Control," *Journal of Guidance, Control, and Dynamics*, Vol. 24, No. 4, 2001, pp. 659–664.

[7]Gurfil, P., "Zero-Miss Distance Guidance Law Based on Line-of-Sight Rate Measurement Only," *Control Engineering Practice*, Vol. 11, No. 7, 2003, pp. 819–832.

[8]Gurfil, P., "Robust Guidance for Electro-optical Missiles," *IEEE Transactions on Aerospace and Electronics Systems*, Vol. 39, No. 2, 2003, pp. 450–461.

[9]Vincent, T. L., and Morgan, R., "Guidance Against Maneuvering Targets Using Lyapunov Optimizing Feedback Control," *Proceedings of the American Control Conference*, IEEE Press, New York, 2002, pp. 215–220.

[10]Yanushevsky, R. T., and Boord, W. J., "A New Approach to Guidance Law Design," AIAA Paper 2003-5577, Aug. 2003.

[11]Singer, R. A., "Estimating Optimal Tracking Filter Performance Manned Maneuvering Targets," *IEEE Transactions on Aerospace and Electronic Systems*, Vol. 6, No. 4, 1970, pp. 473–483.

[12]Shinar, J., Oshman, Y., and Turetsky, V., "On the Need for Integrated Estimation/Guidance Design for Hit-to-Kill Accuracy," *Proceedings*

of the American Control Conference, American Automatic Control Council, Evanston, IL, 2003, pp. 402–407.

[13]Manchester, I. R., and Savkin, A. V., "Circular Navigation Missile Guidance with Incomplete Information and Uncertain Autopilot Model," AIAA Paper 2003-5448, Aug. 2003.

[14]Rusnak, I., "Optimal Guidance Laws with Uncertain Time-of-Flight," *IEEE Transactions on Aerospace and Electronics Systems*, Vol. 36, No. 2, 2000, pp. 721–725.

[15]Khalil, H. K., *Nonlinear Systems*, second ed., Prentice–Hall, Upper Saddle River, NJ, 1996, pp. 211–216.

[16]Chilali, M., and Gahinet, P., "H_∞ Design with Pole Placement Constraints: An LMI Approach," *IEEE Transactions on Automatic Control*, Vol. 41, Vol. 3, 1996, pp. 358–367.

Trajectory Shaping in Linear–Quadratic Pursuit–Evasion Games

Joseph Z. Ben-Asher,* Sergei Levinson,† Josef Shinar,‡ and Haim Weiss§
Technion—Israel Institute of Technology, 32000 Haifa, Israel

I. Introduction

INTERCEPTION of a maneuverable target can be formulated as a zero-sum pursuit–evasion game. For the sake of analytical solvability, there is interest in using a linear game model. Fortunately, in most cases the relative end-game trajectory can be linearized. The nonlinear phenomenon of bounded lateral acceleration can be modeled either by bounded controls or by adding quadratic penalty terms on the (assumed to be unbounded) controls to the square of the miss distance, the natural cost function of the game.[1,2]

The clear advantage of the linear–quadratic formulation is a continuous and smooth linear control strategy, in contrast to the discontinuous (bang–bang) control of the game with bounded controls, at the expense of some increase of the miss distance. In a recent paper,[3] it was shown that by decreasing the pursuer's penalty coefficient, while keeping its ratio to the penalty coefficient of the evader constant, the guaranteed homing accuracies of the linear–quadratic game solution and of the game with bounded controls become similar.

Another advantage of the linear–quadratic differential game (LQDG) formulation is its flexibility, which enables it not only to include in the cost function additional weights on other terminal variables, but also to introduce some "trajectory shaping" by augmenting the cost function with a running-cost (quadratic-integral) term on the state variables. In a very recent study[4] it was discovered that the trajectory-shaping term also leads to attenuation of the disturbance created by random maneuvering of the evader.

In this short Note the effect of the trajectory-shaping term on such disturbance attenuation is presented and analyzed. The model used for the analysis assumes planar geometry, first-order pursuer, and ideal evader dynamics. The analysis leads to a differential Riccati equation that needs to be solved. A simple technique for facilitating the solution is proposed.

The Note is organized as follows: In the next section the standard two-dimensional problem geometry and the mathematical modeling will be reviewed. The problem formulation and analysis by the LQDG theory will be presented in Sec. III. Section IV presents some numerical results including a comparison between the LQDG and the hard-bounded game results. Section V summarizes the paper.

Received 3 April 2004; revision received 6 June 2004; accepted for publication 7 June 2004.

*Associate Professor, Faculty of Aerospace Engineering. Associate Fellow AIAA.

†Graduate Student, Faculty of Aerospace Engineering.

‡Professor Emeritus, Faculty of Aerospace Engineering. Fellow AIAA.

§Adjunct Senior Teaching Fellow and Lady Davis Visiting Scientist; on sabbatical leave from RAFAEL, P.O.B. 2250, Department 35, 31021 Haifa, Israel.

II. Mathematical Modeling

We shall make the following assumptions:

1) The end game is two-dimensional and takes place in the horizontal plane (gravity is compensated for independently).
2) The speeds of the pursuer (the missile) P and the evader (the target) E are constant during the end game (approximately true for short end games).
3) The trajectories of P and E can be linearized around their collision course.
4) The pursuer is more maneuverable than the evader.
5) We assume first-order pursuer and ideal evader dynamics (conservative assumption from the pursuer's point of view).
6) The pursuer can measure its normal acceleration in addition to the relative separation and velocity, and it has an estimate of the time to go.

We assume that the collision condition is satisfied (Fig. 1); namely,

$$V_p \sin(\gamma_{p_0}) - V_e \sin(\gamma_{e_0}) = 0 \tag{1}$$

where V_e and V_p are the pursuer's and evader's velocities and $\gamma_{p_0}, \gamma_{e_0}$ are the pursuer's and evader's nominal heading angles, respectively. In this case, the nominal closing velocity V_c is given by

$$V_c = -\dot{R} = V_p \cos(\gamma_{p_0}) - V_e \cos(\gamma_{e_0}) \approx \text{const} \tag{2}$$

and the (nominal) terminal time is given by

$$t_f = R_0 / V_c \tag{3}$$

where R_0 is the initial length of the line of sight.

Let Y_e, Y_p be the separation (Fig. 1) of the evader and the pursuer, respectively, from the nominal line of sight, and let y be the relative separation (i.e., $y \equiv Y_e - Y_p$), leading to the dynamic equation

$$\dot{y} = \dot{Y}_e - \dot{Y}_p = V_e \sin(\gamma_{e_0} + \gamma_e) - V_p \sin(\gamma_{p_0} + \gamma_p) \tag{4}$$

where γ_p, γ_e are the deviations of the pursuer's and evader's headings from the nominal collision values, respectively. If these deviations are small enough, we may use an approximation to obtain

$$\sin(\gamma_{p_0} + \gamma_p) \approx \sin(\gamma_{p_0}) + \cos(\gamma_{p_0})\gamma_p \tag{5}$$

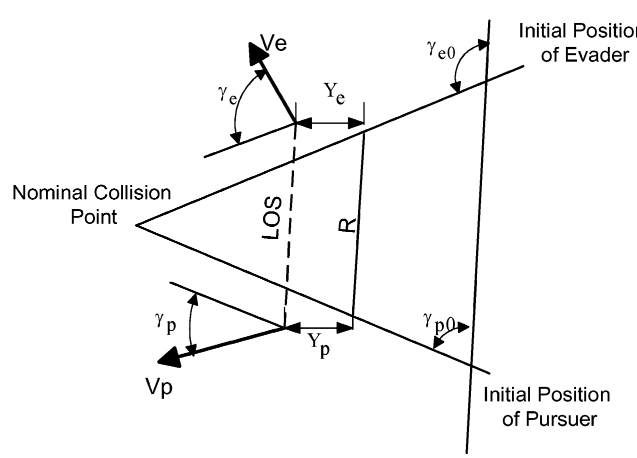

Fig. 1 Problem geometry.